

# Model-Centric and Data-Centric Aspects of Active Learning for Neural Network Models

John Daniel Bossr, Erik Srstadius, Morteza Haghir Chehreghani  
Chalmers University of Technology, Sweden

## Abstract

We study different data-centric and model-centric aspects of active learning with neural network models. i) We investigate incremental and cumulative training modes which specify how the currently labeled data are used for training. ii) Neural networks are models with a large capacity. Thus, we study how active learning depends on the number of epochs and neurons as well as the choice of batch size. iii) We analyze in detail the behavior of query strategies and their corresponding informativeness measures and accordingly propose more efficient querying and active learning paradigms. iv) We perform statistical analyses, e.g., on actively learned classes and test error estimation, that reveal several insights about active learning.

## 1 Introduction

The recent advances in Artificial Intelligence (AI) have been focused on Artificial Neural Network (ANN) models (LeCun, Bengio, and Hinton 2015; Goodfellow, Bengio, and Courville 2016) with great success in pattern recognition (computer vision, NLP) and some reinforcement learning applications (e.g., AlphaGo (Silver et al. 2016)). These models have become popular due to their high flexibility, capacity and accuracy. However, they are data-hungry, i.e., they require a huge amount of labeled data for training. In an image classification task, for instance, the model needs a large training data set possibly in the order of millions images (Goodfellow, Bengio, and Courville 2016). In practice, many applications and tasks might not have access to such a large training data set. In particular, annotating and labeling data is often time consuming, tedious and expensive. Usually, we can not afford to annotate all data, due to a limited budget, and the goal is thus to attain the best gain from this limitation.

The paradigm of choosing the most informative data to label is referred to as *active learning* (Cohn, Ghahramani, and Jordan 1996; Settles 2009). The main challenge is that there is no objectively superior way to determine how informative each data label is. Therefore, active learning is usually performed in the context of sequential decision making, where at every step, two operations are performed: i) choose the next object or data to be labeled and annotated, ii) update the underlying (training) model w.r.t. the new annotation. The next object for labeling is chosen according to a

*query strategy* or an *acquisition function*.<sup>1</sup> The objective is to maximize the test accuracy or minimize its loss, with a minimal number of queries. Common query strategies aim to reduce uncertainty w.r.t. objectives such as *margin*, *variance*, *uncertainty*, *model change* and *entropy* (Settles 2009; Wilson, Hutter, and Deisenroth 2018; Sener and Savarese 2018). The method in (Houlsby et al. 2011) applies predictive entropy to the Gaussian Process Classifier to develop a Bayesian approach for active learning called BALD. This method has been investigated in the context of deep learning too, using some approximate techniques based on drop-out (Gal, Islam, and Ghahramani 2017; Kirsch, van Amersfoort, and Gal 2019).

The queries may be performed in the form of class labels or pairwise relations. Querying class labels is usually more common (Cohn, Ghahramani, and Jordan 1996; Dasgupta, Hsu, and Monteleoni 2000; Gal, Islam, and Ghahramani 2017; Hanneke 2007), which has been extensively used in robotics, text and image classification, medicine, manufacturing and log data analysis (Tong 2001; Yan, Chaudhuri, and Javidi 2018). Querying the pairwise relations has been mainly studied in the context of semi-supervised learning and (supervised/interactive) clustering (Ashtiani, Kushagra, and Ben-David 2016; Awasthi, Balcan, and Voevodski 2017; Awasthi and Zadeh 2010). Noisy active learning has been developed separately for both label-based annotations (Yan, Chaudhuri, and Javidi 2016; Naghshvar, Javidi, and Chaudhuri 2013; Frénay and Verleysen 2014) and pairwise annotations (Mazumdar and Saha 2017; Awasthi, Balcan, and Voevodski 2017), with applications in different areas such as recommendation systems, computer vision, and medicine.

In this paper, we investigate several novel data-centric and model-centric aspects of active learning with neural network models. i) We investigate incremental and cumulative training modes which specify how the available labeled data set is used to train the neural network model. ii) We investigate in detail the behaviour of query strategies (acquisition functions) and their relations to training and test performance. iii) We consider the cases where not all the unlabeled data is available right from at the beginning, or because of compu-

<sup>1</sup>Sequential decision making usually addresses a more complex problem, e.g., finding the correct decision region with an optimal testing policy (Chen et al. 2017).

tational limitations, the acquisition function can be investigated only on a subset (sample) of the entire unlabeled data. We study the behaviour of query strategies in this setting. iv) We study the initial bias a query strategy like entropy might induce when the initial network is not yet trained properly. We suggest random start to address this issue. v) We develop a semi-supervised active learning paradigm by extending the method in (Lee 2013) which enables the model to employ the unlabeled data for a better training, in addition to the labeled data. These studies help us for a better understanding of active learning for neural network models and provide useful guidelines for more effective design of such learning paradigms. In the supplemental, we study several other aspects such as query strategies, performance on different data sets, batch size, etc.

## 2 Background

We are given a set of objects with indices  $\{i\}$  and the respective representations (features)  $\{\mathbf{x}_i\}$ . The true label of object  $i$  is indicated by  $y_i$  which might be given or not. Thus, we consider two data sets  $L$  and  $U$ , where  $L$  includes the object whose true labels are known whereas  $U$  consists of unlabeled objects. We may consider a separate test data set to evaluate and compute the test accuracy of the trained models. Given an input  $\mathbf{x}_i$  to a neural network  $C$ , we obtain the softmax outputs (predictive class probabilities)  $\hat{y}_{ic}$  for object  $i$ .  $\hat{y}_{ic}$  indicates the probabilistic prediction  $P_C(\hat{y} = c|\mathbf{x}_i)$ , i.e., the probability that  $i$  belongs to class  $c$ . A query strategy  $A$  assigns an informativeness measure  $I_i^A$  to every  $i$  in the unlabeled data set  $U$ . The query strategy then sorts the unlabeled objects based on  $I_i^A$  and selects a batch  $B$  consisting of  $n$  objects with the highest  $I_i^A$  ( $n$  is the batch size and is fixed in advance).

$$B = \{B_1, \dots, B_n\}, \quad \text{s.t.} \quad I_{B_1}^A \geq I_{B_2}^A \geq \dots \geq I_{B_n}^A \\ \text{and} \quad I_{B_n}^A \geq I_i^A \quad \forall i \in U \setminus B.$$

For each object in  $B$ , we ask the oracle (that can be for example an expert) to provide a class label. We then update the set of all labeled data by  $L \leftarrow L \cup B$  and the set of all unlabeled data by  $U \leftarrow U \setminus B$ . Sometimes we might need to compute the mean informativeness measure  $\bar{I}_B^A$  of the query strategy  $A$  for the selected batch  $B$  as  $\bar{I}_B^A = \frac{1}{|B|} \sum_{i \in B} I_i^A$ .

The main query strategies used this paper, i.e. *Random*, *Margin*, and *Entropy*, only differ in the way they assign their corresponding informativeness measures.

**Random (R)** assigns a uniformly distributed informativeness measure  $I_i^R \sim \text{unif}(0, 1)$  to all  $i \in U$ .

**Margin (M)** computes informativeness measures for each object  $i \in U$  as  $I_i^M = -[P_C(\hat{y} = \tilde{c}_1|\mathbf{x}_i) - P_C(\hat{y} = \tilde{c}_2|\mathbf{x}_i)]$ , where  $\tilde{c}_1$  and  $\tilde{c}_2$  are the most probable and the second most probable classes predicted by classifier  $C$  for  $i \in U$ .

**Entropy (E)** assigns the informativeness measure based on the entropy of the predictive distribution, i.e.,  $I_i^E = -\sum_c P_C(\hat{y} = c|\mathbf{x}_i) \log P_C(\hat{y} = c|\mathbf{x}_i)$ .

**Neural network architectures and models.** We use the MNIST (LeCun and Cortes 2010), Fashion-MNIST (Xiao,

Rasul, and Vollgraf 2017) and CIFAR-10 (Krizhevsky 2012) data sets for training and evaluation of the networks in different active learning paradigms. There are 70000 images in MNIST and Fashion-MNIST, where each image consists of  $28 \times 28$  features. CIFAR-10 contains 60000 images with  $32 \times 32 \times 3$  features. 10000 images from each data set are reserved as a test set. The same network is used for both the MNIST and Fashion-MNIST data sets and is referred to as  $\text{ANN1}_{m,e}$ . The network consists of three layers with  $m$  neurons in the hidden layer and  $e$  is the number of epochs. For the CIFAR-10 data set, we use a convolutional neural network consisting of several layers that uses 50 epochs, which we refer to as  $\text{CNN1}$ . The pseudocode for both types of networks can be found in the supplemental.

## 3 Query Strategies and Training Modes

**Methodology.** Design of an effective query strategy constitutes a core component of any active learning paradigm. Different query strategies have been well investigated in several studies, for example in (Settles 2009; Wilson, Hutter, and Deisenroth 2018; Sener and Savarese 2018). However, after querying the label of a new object, the underlying model  $C$  should be updated accordingly. In this section, we study two modes of updating the model, where we call them *incremental training* and *cumulative training*.

i). *Incremental training*: We consider the trained model on the previously labeled objects  $L$  and update its parameters (i.e., the weight and bias parameters of the neural network) only using the new labeled batch  $B$ .

ii). *Cumulative training*: We re-initialize the weight and bias parameters of the model and use  $L \cup B$  for training.

Incremental training is usually faster and computationally more efficient. However, the incremental mode induces a certain order on the way the labeled data is fed into the network which might yield some bias. The cumulative method, on the other hand, utilizes the entire labeled data set at each acquisition step and thus induces randomness to the training order. Computational runtime might not be the main objective in active learning as its goal is to minimize the number of queries to the oracle.

Active learning methods usually use the incremental training mode. The cumulative training has not been well studied in this context. In this section, we study combinations of query strategies and training modes for a large neural network model. We use  $\text{ANN1}_{100,1}$  neural networks to perform the experiments on MNIST and Fashion-MNIST data sets. We choose a batch size of 120 objects. We also investigate the effects of selecting data with one network, and training another network with the already selected data. These two networks, i.e., the *selection network* and *evaluation network*, might differ in the number of epochs and neurons. This separation of networks helps us to study if the difference in results is due to the specific training modes, or it is because of the different labeled data selected in each of the settings.

**Results and discussion.** Figures 1a and 1b show the test accuracy of the networks for different ratios of the labeled data, where 100% corresponds to the case where the whole

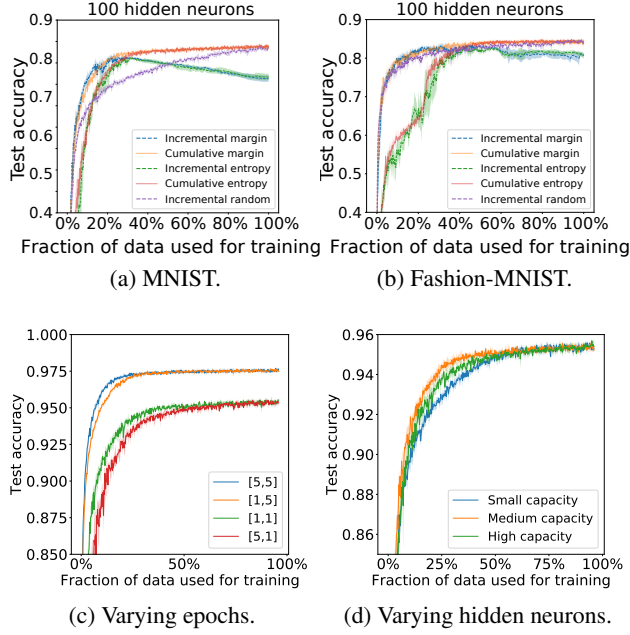


Figure 1: Test accuracy for  $\text{ANN}_{100,1}$  network on the MNIST (a) and Fashion-MNIST (b) data sets. In (c) we vary the number of epochs in the selection and evaluation network. Figure (d) shows the test accuracy for varying number of hidden neurons in the selection network. The results in (c) and (d) are on the MNIST data set.

unlabeled data set of 60000 images has been labeled and used for training. We report the results for different choices of query strategies and training modes. With random query strategy, the results for the cumulative and incremental training modes are very similar, thus we report only the results of incremental mode.

In Figures 1a and 1b we observe that the margin query strategy initially outperforms both the random and the entropy query strategies in both of the training modes. In the supplemental, we investigate other strategies and several network capacities, where we again observe the superior performance of the margin query strategy. This observation is consistent with the prior studies with other models than neural network (Körner and Wrobel 2006). Comparison of query studies has been studied in several other works with consistent observations, thus we will not focus a lot in this paper. Thereby, in most of our studies, we will use the margin query strategy. In addition, we observe that the entropy query strategy performs similarly and sometimes even worse than the random strategy at the beginning, which might be due to the bias induced by this specific query strategy. In Section 6 we study this effect and a method to mitigate it.

An even more important observation is that the cumulative training performs better than the incremental training, in particular when the size of the labeled data is not too small. For the MNIST data set, the incremental and the cumulative modes perform similarly up to 10000 images labeled and used in training. After that, cumulative mode starts outper-

forming. The networks trained in the incremental mode experience a decline in test accuracy after a certain number of objects have been labeled. This is probably due to the bias induced by the order of the data processing that the incremental mode yields. The training order is randomized with the cumulative mode which has access to all the labeled data randomly via stochastic gradient descent.

In summary, margin query strategy with incremental training outperforms the alternatives initially. The cumulative mode yields better results throughout the training process, in particular when a large fraction of the data has been already labeled.

Figure 1c shows the test accuracy of the evaluation network while varying the number of epochs in the networks. The legend  $[a, b]$  means that  $\text{ANN}_{100,a}$  and  $\text{ANN}_{100,b}$  are used as the selection and evaluation networks respectively. Figure 1d shows the test accuracy of the  $\text{ANN}_{100,1}$  evaluation network. The selection network is either  $\text{ANN}_{10,1}$  (Small),  $\text{ANN}_{100,1}$  (Medium) or  $\text{ANN}_{1000,1}$  (High). Both Figures 1d and 1c imply that it is always beneficial to have the same number of epochs and neurons for the selection and evaluation networks. Therefore, the evaluation network should be decided before selecting data, since the selection and evaluation networks should have the same number of epochs and neurons.

## 4 Informativeness Measures

**Methodology.** Different query strategies usually assign an informativeness measure to unlabeled data. In this study, we investigate how the informativeness measures relate to how quickly the performance (accuracy) of the network improves. For example, at some point labeling new data may be expensive compared to the improvement in test accuracy. We thus study if the training accuracy and informativeness measure may be used to evaluate the current state of the network, i.e., we formulate a stopping criterion for labeling (querying) without the need for a dedicated test set.

It can be difficult to compare informativeness measures from different query strategies since they have different interpretations and ranges. Thus, to determine the informativeness of different batches, we use the same informativeness measure, independent of how the batch is sampled. In this study we focus on the informativeness measure associated with random sampling  $R$  and the cumulatively trained margin query strategy  $M$ . These choices are consistent with the results from Section 3. The *margin on random informativeness measure* (MOR) is obtained by the mean margin informativeness measure  $\bar{I}_B^M$  on a randomly selected batch  $B$  with a network trained on the randomly selected data  $L$ .

**Results and discussion.** Figure 2 shows how the test accuracy, the train accuracy and  $\bar{I}_B^M$  change while training with a query strategy. The results are obtained with cumulative training with a batch size of 120. The figure shows the results for the three data sets MNIST, Fashion-MNIST and CIFAR10, where we have used  $\text{ANN}_{100,1}$ ,  $\text{ANN}_{100,1}$  and  $\text{CNN1}$  networks respectively.

We observe that the query strategy  $M$  yields a higher test accuracy, a lower train accuracy, and the respective  $\bar{I}_M^B$  is

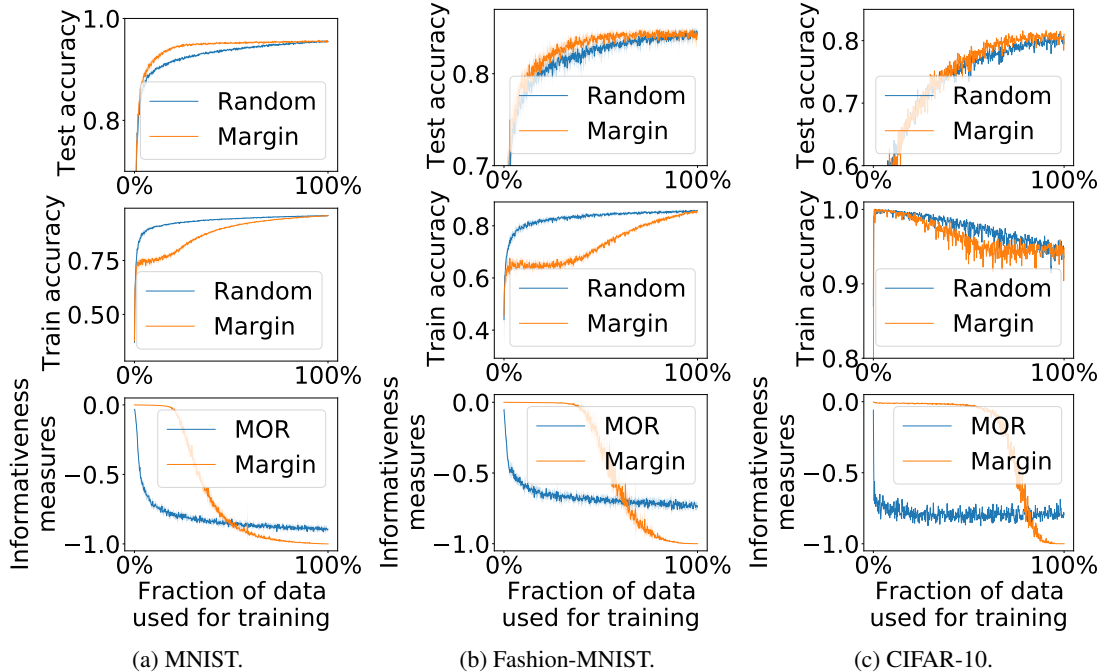


Figure 2: Test accuracy, training accuracy, and  $\bar{I}_B^M$  measure for query strategies  $M$  and  $R$ .

higher during the early steps of training, compared to the MOR measure that uses  $R$ . Interestingly, with margin query strategy, we sometimes obtain a higher test accuracy compared to its training accuracy. It is usually expected that classifiers optimized on training sets have higher training accuracy than test accuracy on an equally distributed test set (James et al. 2013, p. 31). This suggests that the test and train sets are not equally distributed. Seeing a lower training accuracy than test accuracy could be interpreted as the margin query strategy actively selects “difficult” objects for labeling and training, and thus the train accuracy is lower. However, the data that the margin query strategy selects is seemingly better for describing the distribution of the test set, indicated by the fact that it yields a higher test accuracy compared to the  $R$  strategy. Thus, to ensure a maximal test accuracy using as few objects as possible, we want the  $\bar{I}_B^M$  to be high. Furthermore,  $\bar{I}_B^M$  can be linked to learnability of the network in the sense that a high  $\bar{I}_B^M$  yields a good improvement in the test accuracy. This means that a decreasing  $\bar{I}_B^M$  can be interpreted as either: (a) an indication that we are not gaining enough accuracy by querying the oracle for labels in the training set and should stop training the network, or, (b) more unlabeled data should be acquired in order to improve accuracy. These observations can be useful in the cases no test set is available to measure the test accuracy.

We also notice the correlation between the increase in train accuracy and the decrease in  $\bar{I}_B^M$ . We may interpret it in two ways: (a) The network learns to characterize the data, which makes the network more certain in its predictions of the objects in  $B$ , thus  $\bar{I}_B^M$  is decreasing. (b) The unlabeled data set  $U$  is depleted of (informative) objects close to the

decision boundaries, since they have a higher  $I_i^M$  and are thus found earlier in the training. The objects that are left are further away from the decision boundaries, and hence, have a lower  $I_i^M$ . We study this behavior in more detail in Section 5.

The training accuracy on the CIFAR-10 data set evolves differently compared to MNIST and Fashion-MNIST, as seen in Figure 2c. The training accuracy starts from a high value and decreases as more data is labeled and used for training, independent of the query strategy used. This is possibly due to training the network with 50 epochs which implies the (small) training set at the beginning can be almost perfectly described by the weights (and the relatively high capacity). We see a slightly better performance in test accuracy when using  $M$  compared to  $R$  after around 50% of the data has been used for training. The observations regarding the  $\bar{I}_B^M$  are consistent for all the examined data sets.

## 5 Data Split and Sampling

**Methodology.** Evaluating query strategies on the entire unlabeled data set  $U$  can be computationally expensive. On the other hand, it might be possible that more unlabeled data is available after active labeling has begun. Therefore, in this section, we study the setting wherein the full  $U$  is not accessible for query strategies. In particular, we first investigate sampling (splitting) unlabeled data along with labeling with active learning. Then we study why the informativeness measure decreases when using the margin query strategy. As illustrated in Figure 2, during the later steps of the training, when almost all the data has been labeled,  $\bar{I}_B^M$  decreases. There are two hypotheses to explain the decrease of  $\bar{I}_B^M$ : (1)

the network learns enough, such that it reaches its best performance and no further improvement is possible; (2) when selecting data with a query strategy, the most informative objects are labeled first, leaving uninformative objects in  $U$ . This means that the decrease of  $\bar{I}_B^M$  is due to exhaustion of informative data. It is likely that both hypotheses contribute to the decrease of  $\bar{I}_B^M$ , but the extent might be different.

If hypothesis (2) is true, then it would be useful to ensure that  $U$  is as large as possible and extend it when the informativeness measure decreases. To understand this, we split the unlabeled data set into  $d$  subsets, i.e.  $U_1, \dots, U_d$ , which are independently and identically distributed. The margin query strategy queries a fraction  $p$  of objects from  $U = U_1$  to be labeled actively and moved to  $L$ . We then use the next unlabeled subset, i.e.  $U \leftarrow U \cup U_2$ . We perform this procedure sequentially for all the  $d$  subsets. In particular, we perform two types of experiments with the following parameters on both the MNIST and Fashion-MNIST data sets.

$d$	$p$	batch size	number of samples in each subset
2	80%	120	30000
5	90%	200	12000

In this setup, the increase in  $\bar{I}_B^M$  upon adding a new subset  $U_j$  is an indication of depletion of informative data in the current  $U$ .

**Results and discussion.** Figure 3 shows the test accuracy and mean informativeness measure  $\bar{I}_B^M$  for different experimental settings. The result corresponding to “Complete data set” is provided for a comparison with having access to all unlabeled data from the beginning. In Figure 3, we observe sharp phase transitions in  $\bar{I}_B^M$  that correspond to drastic increase of  $\bar{I}_B^M$  upon adding every new subset to  $U$ . Even with the last subset in Figures 3c and 3d, where the model is already trained using 43,200 objects,  $\bar{I}_B^M$  instantly increases from -1 to 0. This observation suggests that the decrease of  $\bar{I}_B^M$  seen in Figure 2 is mainly because the unlabeled data set does not contain informative objects anymore.

We also observe the increase of the test accuracy as new subsets are added to  $U$ , as shown in Figures 3a and 3c. This is in particular more significant when  $\bar{I}_B^M$  is high. This reinforces the idea that the rate of increase in test accuracy is related to the  $\bar{I}_B^M$ , as discussed in Section 4. The more informative the data is, the faster the increase in accuracy occurs. We also observe in Figure 3 that it would be preferable to have access to all the unlabeled data from the beginning compared to gathering them during the active learning process. The test accuracy when all the data is available is always higher.

The phase where  $\bar{I}_B^M$  is close to 0 is the longest when  $U_1$  is added. It becomes shorter for each new subset added as shown in Figure 3. As the network gets more trained, the number of batches with approximately zero  $\bar{I}_B^M$  decreases. Therefore, from the results illustrated in Figure 3 we conclude that  $\bar{I}_B^M$  is high as long as there are informative objects in the unlabeled set  $U$ . This is consistent with the observation in Figure 2 showing that the training accuracy increases faster when  $\bar{I}_B^M$  is high.

## 6 Random Start

**Methodology.** When we start active learning, at the beginning, the network is not trained properly. Thus, the model predictions might be inaccurate. This means that the first batch selected by a query strategy might be biased towards a certain class, in particular if the network is initialized randomly. To investigate if such a bias exists, we examine the number of occurrences of the different classes that the query strategies select. We do this by initializing an ANN<sub>100,1</sub> network and letting it select 1000 images using a query strategy. This procedure is repeated 200 times where we examine the  $M$  and  $E$  query strategies and compare them to  $R$ .

Our hypothesis is that the query strategies might be biased towards dark images. We explore this idea by generating images of size  $28 \times 28$  pixels containing uniformly random noise. A certain percentage  $\alpha$  of the pixels, selected randomly, are turned black. If the images with  $\alpha$  close to 1 have higher  $I_i^A$ , we conclude that the query strategy  $A$  is biased. We repeat this 100 times using a randomly initialized ANN<sub>100,1</sub> network.

We then argue that the bias effect can be mitigated by sampling with  $R$  initially. We refer to this as a *random start*. The *random start size* is the number of objects that are selected randomly for labeling. We perform an experiment with a random start sizes of 2000 with a cumulatively trained ANN<sub>100,1</sub> network to see if the random start yields any performance benefits. A random start size of 200 is examined in the supplemental.

**Results and discussion.** Figure 4 (first row) shows the box-plots of the class occurrences for the Fashion-MNIST data set with the  $M$ ,  $E$  and  $R$  query strategies. The class distribution of the objects selected by  $R$  is consistent with the distribution of the entire data set. The query strategies  $M$  and  $E$  select objects in a way that the class 5 tends to be over-represented, corresponding to the images of *Sandals*. This observation is even more obvious when using  $E$ . We thus conclude that the query strategies might be biased in their selection when performing on an untrained network.

Figure 4 (second row) shows how  $I_i^A$  changes depending on  $\alpha$ , averaged over 100 runs.  $I_i^A$  increases with  $\alpha$  for  $M$  and  $E$  strategies.  $M$  shows a relatively large variance compared to  $E$ , which possibly explains why its class distribution is closer to uniform in Figure 4e. Intuitively, an image of a “Sandal” should be darker compared to the other classes, such as “T-shirt” or “Coat” in the Fashion-MNIST data set, due to its smaller surface area and the background being dark. Figures 4e and 4f thus explain why class 5 is over-represented in the first batch. We guess the preference for darker images is mostly due to the combination of the initialization and the specific form of the query strategies.

Figure 5a illustrates the test accuracy with a random start of size 2000 for the entropy query strategy, which yields a significant performance improvement. A random start of size 200 was also tested, which can be seen in the supplemental. With a smaller random start size of 200 we do not observe a significant improvement. The size is insufficient to obtain a reliable initial training of the network in order to mitigate the bias.

Additionally, as a side study, we investigate the random

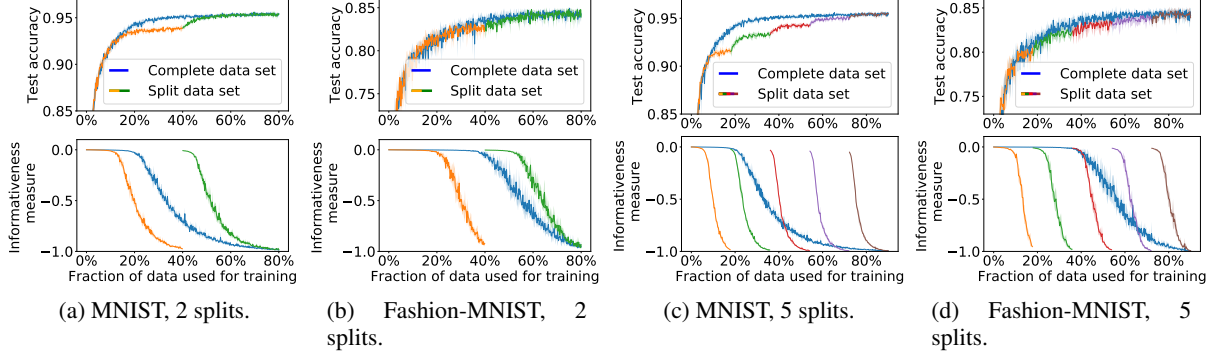


Figure 3: The effect of data splits on the informativeness measure and test accuracy when new unlabeled subsets are added during active learning.

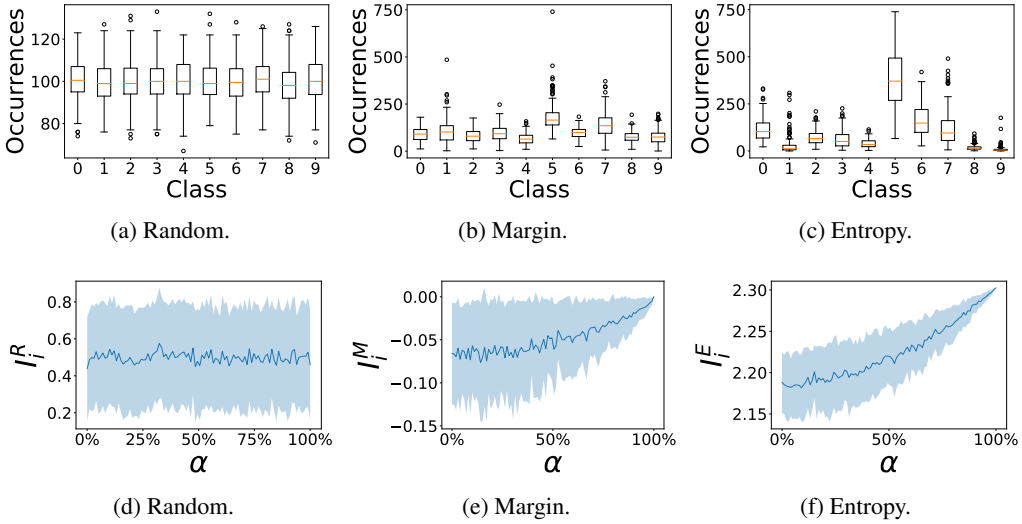


Figure 4: Class distributions and  $I_i^A$  as a function of  $\alpha$ .

start to compute heuristic empirical lower and upper bounds on the test accuracy. This can in particular be useful when a separate labeled test data set is not available for evaluations. We consider the following test and training sets for this purpose. i)  $L_t$ : contains the random start objects and is used as a test set. ii)  $\underline{L}$ : contains all labeled objects excluding the random start, i.e., only the objects labeled via the margin query strategy. iii)  $L = L_t \cup \underline{L}$ : includes all labeled data. We obtain the empirical lower bound on test accuracy by training the model on  $\underline{L}$  and evaluating on  $L_t$ . We obtain the empirical upper bound by training on  $L$  and evaluating on  $L_t$ , which means that the test set is a subset of the training set. Figure 5b shows that the test accuracy of an  $\text{ANN}_{100,5}$  network on MNIST lies between the heuristic empirical lower and upper bounds, using a random start size of 3000. A varying number of epochs and random start sizes are investigated in the supplemental.

## 7 Semi-Supervised Deep Active Learning

**Methodology.** In active learning, it is often assumed that unlabeled data is abundant. So far, in this paper, we have assumed that only the labeled data is used to train a neural network. In this section, we investigate if semi-supervised learning can be used in conjunction with active learning, to benefit from unlabeled data.

For this purpose, we extend the semi-supervised learning method in (Lee 2013), where the network assigns *pseudo-labels* to the unlabeled data, and they also contribute to train the network. For each object, the assigned pseudo-label is the most probable class according to the prediction made by the network. This method yields an effective way to use semi-supervised training with deep neural networks. Our extension involves the use of informativeness measures to assess the confidence of the network predictions. In this way, we repeatedly assign those pseudo-labels to unlabeled data that the model is confident about to minimize errors. We call this method the *Gradual Pseudo-Labeling Algorithm*.



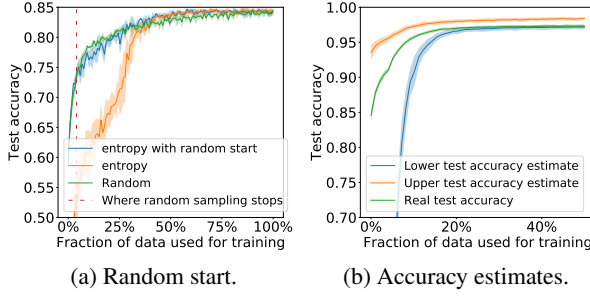


Figure 5: Test accuracy improvement with random start (a) and estimates of test accuracy (b) when using random start.

(GPLA).

**The Gradual Pseudo-Labeling Algorithm (GPLA).** We perform GPLA after a network has been trained using some labeled data  $L$ . For every object  $i \in U$ , the probability estimates  $\hat{y}_{ic}$  are computed for every class  $c$  by feeding the data  $\mathbf{x}_i$  through the neural network. The probability estimates  $\hat{y}_{ic}$  are then used in conjunction with the least confident informativeness measure  $I_i^{LC} = -\max_c P_C(y = c | \mathbf{x}_i)$  to determine the confidence of the network in predictions. We then construct the *confident subset*  $S_\xi$  defined as  $S_\xi = \{i \in U \mid I_i^{LC} < \xi\}$  where  $\xi$  is the *confidence threshold*. We assign to every  $i \in S_\xi$  a pseudo-label that matches the predicted class  $\arg \max_c \hat{y}_{ic}$ . We then update the set of all labeled data by  $L \leftarrow L \cup S_\xi$  and the set of all unlabeled data by  $U \leftarrow U \setminus S_\xi$ . We retrain the network with the newly extended data set  $L$  and the process is repeated until only very few objects are added to  $S_\xi$ . As the network becomes more confident in its predictions, we add more pseudo-labels, hence we call it *gradual* pseudo-labeling. Algorithm 1 summarizes the different steps of the procedure.

---

**Algorithm 1:** The *Gradual Pseudo-Labeling Algorithm* (GPLA), given a confidence threshold  $\xi$  and fewest allowed points  $N$  in  $S_\xi$ .

---

- 1 Train network  $C$  using all labeled data in  $L$ .
  - 2 Obtain  $\hat{y}_{ic}$  by feeding  $\mathbf{x}_i$  to  $C$ , for every  $i \in U$ .
  - 3 Compute  $I_i^{LC}$  for every  $i \in U$ .
  - 4 Construct  $S_\xi = \{i \in U \mid I_i^{LC} < \xi\}$ .
  - 5 **if**  $|S_\xi| > N$  **then**
  - 6     Get the pseudo-labels by  $\arg \max_c \hat{y}_{ic}$  for every  $i \in S_\xi$ .
  - 7      $L \leftarrow L \cup S_\xi, U \leftarrow U \setminus S_\xi$ .
  - 8     Repeat from step 1 until  $|S_\xi| \leq N$ .
- 

**Finding a suitable threshold.** The threshold  $\xi$  may have a significant impact on the semi-supervised learning scheme. A too hard threshold, i.e., a  $\xi \gtrsim -1$ , makes  $S_\xi = \emptyset$ , which would be equivalent to only performing supervised active learning. On the other hand, a too soft threshold, i.e.,  $\xi \lesssim 0$ , causes  $S_\xi = U$ , which could be suboptimal. We hypoth-

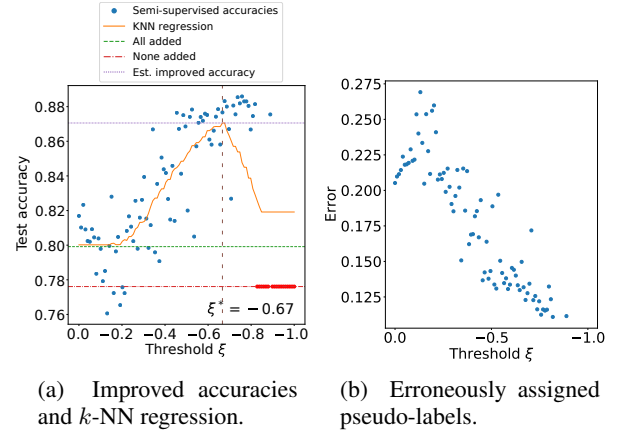


Figure 6: Test accuracy and pseudo-labeling assignment error after using GPLA.

esize that there exists an optimal threshold  $\xi^*$  which yields the best performance for GPLA given the current state of the network. We find a proper  $\xi$  by first performing GPLA using several candidate thresholds  $\xi \in [-1, 0]$  and measuring the corresponding test accuracy of the network. We perform a  $k$ -NN ( $k$  nearest neighbor) regression as a function of the threshold values and select the  $\xi$  that gives the highest accuracy in the regression. Note that in principle one can use any other suitable regression model, instead of  $k$ -NN regression.

**Experimental setup.** We train an  $\text{ANN}_{1_{n,e}}$  network cumulatively on the data selected by a query strategy  $A$ . When a certain number  $p$  of unlabeled objects are labeled by the oracle through the query strategy, the optimal threshold  $\xi^*$  is found for the network by testing 100 uniformly distributed thresholds between -1 and 0. We apply the  $k$ -NN regression with  $k = 30$ . While evaluating the thresholds, we also consider the number of erroneously labeled objects to investigate if the number of errors the algorithm makes changes depending on  $\xi$ . Given  $\xi^*$ , we then employ GPLA to obtain the new test accuracy using  $N = 150$ . Training of GPLA is done in the cumulative mode.

The number of examined labeled images  $p$  is equal to 500, 1000, 2500, 5000, 10000, 20000, and 50000, where there are 60000 images in total. We choose the query strategy  $A$  to be either  $M$  or  $R$ . We use an  $\text{ANN}_{100,1}$  network for the MNIST data set to evaluate the usefulness of GPLA. Further results on other data sets and models are reported in the supplemental.

**Results and discussion.** Figure 6a shows the results w.r.t. the threshold  $\xi$  for  $p = 1000$ , where we observe improvement in the test accuracy with semi-supervised learning for the 100 candidate thresholds  $\xi \in [-1, 0]$ . The network is  $\text{ANN}_{100,1}$  trained with the margin query strategy. As the thresholds get harder (that is, closer to -1) we see an improvement in test accuracy, i.e., an almost (negative) correlation between the threshold and the test accuracy. The result indicated by 'All added' is the average test accuracy for all  $\xi$  for which  $S_\xi = U$ , i.e., the runs wherein all the objects

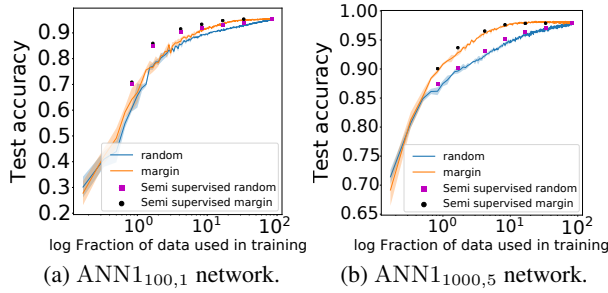


Figure 7: Test accuracy before and after semi-supervised active learning.

are assigned a pseudo-label at the first iteration. Thus it corresponds to the way the pseudo-labels are assigned in (Lee 2013). Figure 6b shows the fraction of erroneously assigned pseudo-labels for different thresholds. Consistently, we observe an almost (positive) correlation between the threshold and the fraction of erroneously assigned pseudo-labels (except for  $\xi$  close to zero). This supports our hypothesis that introducing a threshold may reduce the number of erroneously assigned pseudo-labels. The choice of  $\xi = -0.8$  almost halves the number of errors, compared to the no threshold case ( $\xi = 0$ ).

Figure 6 suggests that the optimal threshold  $\xi^*$  is the hardest (smallest) threshold that still allows the network to assign pseudo-labels, i.e., a threshold for which  $S_\xi \neq \emptyset$ . Thus, in principle, one may avoid using  $k$ -NN regression, and a validation set, to select a proper  $\xi$ . Such a choice makes sense since a hard threshold suggests choosing only very confident pseudo-labels. Then, by repeating the procedure possibly new confident pseudo-labels are obtained. Therefore, at the end, we compute all the confident pseudo-labels obtained through either the true labels or the other confident pseudo-labels, and together with true labels, we use them for training the network. The test accuracy in Figure 6a increases from 78% to 88%, after applying the gradual pseudo-labeling assignment with the hardest  $\xi$ , when 1000 images from in total 60000 images are labeled by the oracle.

Figure 7 shows the test accuracy before and after pseudo-labeling is applied. We observe that the semi-supervised test accuracy is higher regardless of whether we use  $M$  or  $R$  for query strategy. The relative increase in accuracy is larger for smaller  $p$ 's. It is natural that the accuracy for a large  $p$  can not be improved much, since the network is almost as good as it can be given correct labels. Therefore, the proposed semi-supervised learning scheme can be used in combination with different query strategies, to be applied after every active learning step to attain the full potential of the unlabeled data set and improve the test accuracy. The improvement in test accuracy can be significant. We note that our approach even potentially allows us to perform semi-supervised learning during the active learning step, making the model more certain about which data to query next.

## 8 Conclusion

We studied in a consistent way several data-centric and model-centric aspects of active learning for neural network models. Our studies provide further insights on this task and help us for a better understanding of the concerns that might arise when using active learning to train a neural network model, e.g., training mode, query strategies, availability of unlabeled data, initial training, and network specifications. We finally investigated semi-supervised active learning via propagating and using pseudo-labels.

## Acknowledgement

This work was partially supported by the Wallenberg AI, Autonomous Systems and Software Program (WASP) funded by the Knut and Alice Wallenberg Foundation.

## References

- Ashtiani, H.; Kushagra, S.; and Ben-David, S. 2016. Clustering with Same-Cluster Queries. In *Advances in Neural Information Processing Systems (NIPS)*, 3216–3224.
- Awasthi, P.; Balcan, M. F.; and Voevodski, K. 2017. Local algorithms for interactive clustering. *Journal of Machine Learning Research* 18(3): 1–35.
- Awasthi, P.; and Zadeh, R. B. 2010. Supervised Clustering. In *Advances in Neural Information Processing Systems (NIPS)*, 91–99.
- Chen, Y.; Renders, J.; Chehreghani, M. H.; and Krause, A. 2017. Efficient Online Learning for Optimizing Value of Information: Theory and Application to Interactive Troubleshooting. In *Proceedings of the Thirty-Third Conference on Uncertainty in Artificial Intelligence (UAI)*.
- Cohn, D. A.; Ghahramani, Z.; and Jordan, M. I. 1996. Active Learning with Statistical Models. *J. Artif. Intell. Res.* 4: 129–145.
- Dasgupta, S.; Hsu, D. J.; and Monteleoni, C. 2000. A general agnostic active learning algorithm. In *Advances in Neural Information Processing Systems 20, Proceedings of the Twenty-First Annual Conference on Neural Information Processing Systems (NIPS)*, 353–360.
- Frénay, B.; and Verleysen, M. 2014. Classification in the Presence of Label Noise: A Survey. *IEEE Transactions on Neural Networks and Learning Systems* 25: 846–869.
- Gal, Y.; Islam, R.; and Ghahramani, Z. 2017. Deep Bayesian Active Learning with Image Data. In *Proceedings of the 34th International Conference on Machine Learning (ICML)*, 1183–1192.
- Goodfellow, I.; Bengio, Y.; and Courville, A. 2016. *Deep Learning*. MIT Press. <http://www.deeplearningbook.org>.
- Hanneke, S. 2007. A bound on the label complexity of agnostic active learning. In *Proceedings of the Twenty-Fourth International Conference on Machine Learning (ICML)*, 353–360.
- Houlsby, N.; Huszár, F.; Ghahramani, Z.; and Lengyel, M. 2011. Bayesian Active Learning for Classification and Preference Learning URL <http://arxiv.org/abs/1112.5745>.



James, G.; Witten, D.; Hastie, T.; and Tibshirani, R. 2013. *An Introduction to Statistical Learning: with Applications in R*. Springer. URL <https://faculty.marshall.usc.edu/gareth-james/ISL/>.

Kingma, D. P.; and Ba, J. 2015. Adam: A Method for Stochastic Optimization. In Bengio, Y.; and LeCun, Y., eds., *3rd International Conference on Learning Representations, ICLR*.

Kirsch, A.; van Amersfoort, J.; and Gal, Y. 2019. Batch-BALD: Efficient and Diverse Batch Acquisition for Deep Bayesian Active Learning. In *Advances in Neural Information Processing Systems 32: Annual Conference on Neural Information Processing Systems (NeurIPS)*, 7024–7035.

Körner, C.; and Wrobel, S. 2006. Multi-class Ensemble-Based Active Learning. In Fürnkranz, J.; Scheffer, T.; and Spiliopoulou, M., eds., *Machine Learning: ECML 2006*, 687–694. Springer Berlin Heidelberg.

Krizhevsky, A. 2012. Learning Multiple Layers of Features from Tiny Images. *University of Toronto*.

LeCun, Y.; Bengio, Y.; and Hinton, G. E. 2015. Deep learning. *Nature* 521(7553): 436–444.

LeCun, Y.; and Cortes, C. 2010. MNIST handwritten digit database URL <http://yann.lecun.com/exdb/mnist/>.

Lee, D.-H. 2013. Pseudo-Label : The Simple and Efficient Semi-Supervised Learning Method for Deep Neural Networks. *ICML 2013 Workshop : Challenges in Representation Learning (WREPL)*.

Mazumdar, A.; and Saha, B. 2017. Clustering with Noisy Queries. In *Advances in Neural Information Processing Systems (NIPS)*, 5788–5799.

Naghshvar, M.; Javidi, T.; and Chaudhuri, K. 2013. Extrinsic Jensen-Shannon divergence and noisy Bayesian active learning. In *51st Annual Allerton Conference on Communication, Control, and Computing (Allerton)*, 1128–1135.

Sener, O.; and Savarese, S. 2018. Active Learning for Convolutional Neural Networks: A Core-Set Approach. In *6th International Conference on Learning Representations, ICLR*.

Settles, B. 2009. Active Learning Literature Survey. Computer Sciences Technical Report 1648, University of Wisconsin–Madison.

Silver, D.; Huang, A.; Maddison, C. J.; Guez, A.; Sifre, L.; van den Driessche, G.; Schrittwieser, J.; Antonoglou, I.; Panneershelvam, V.; Lanctot, M.; Dieleman, S.; Grewe, D.; Nham, J.; Kalchbrenner, N.; Sutskever, I.; Lillicrap, T. P.; Leach, M.; Kavukcuoglu, K.; Graepel, T.; and Hassabis, D. 2016. Mastering the game of Go with deep neural networks and tree search. *Nature* 529(7587): 484–489.

Tong, S. 2001. *Active learning: theory and applications*. Stanford University.

Wilson, J. T.; Hutter, F.; and Deisenroth, M. P. 2018. Maximizing acquisition functions for Bayesian optimization. In *Advances in Neural Information Processing Systems 31 (NIPS)*, 9906–9917.

Xiao, H.; Rasul, K.; and Vollgraf, R. 2017. Fashion-MNIST: a Novel Image Dataset for Benchmarking Machine Learning Algorithms. *CoRR* abs/1708.07747. URL <http://arxiv.org/abs/1708.07747>.

Yan, S.; Chaudhuri, K.; and Javidi, T. 2016. Active Learning from Imperfect Labelers. In *Advances in Neural Information Processing Systems (NIPS)*, 2128–2136.

Yan, S.; Chaudhuri, K.; and Javidi, T. 2018. Active Learning with Logged Data. In *Proceedings of the 35th International Conference on Machine Learning (ICML)*, 5517–5526.

## A Further Studies

### A.1 Other Query Strategies

In addition to the query strategies in Section 3, we examine the performance of two additional query strategies: the *Least Confident* (LC), and *Least Squares* (LS) strategies, with the corresponding informativeness measures  $I_i^{LC} = -\max_c P_C(y = c | \mathbf{x}_i)$  and  $I_i^{LS} = -\sum_c [P_C(y = c | \mathbf{x}_i) - \frac{1}{N_c}]^2$ . Figure 8 shows their performance in relation to the random query strategy using the cumulative and incremental training modes. We observe that the performance of *LC* and *LS* is similar to the performance of *E* in Figure 1.

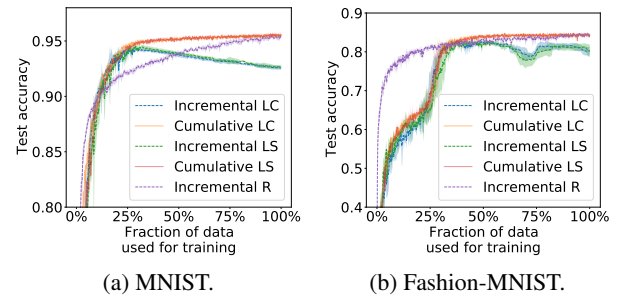


Figure 8: Test accuracy of ANN<sub>100,1</sub> on the MNIST (a) and Fashion-MNIST (b) data sets, with the least confident and least squares query strategies.

### A.2 Effect of Cumulative and Incremental Modes on $\bar{I}_B^M$ .

Figure 9 illustrates the  $\bar{I}_B^M$  of the selected batches for both incremental and cumulative training modes. These results correspond to the results shown in Figures 1a and 1b. We observe that  $\bar{I}_B^M$  decreases after 20% of all MNIST data has been used in training, or at 40% in the Fashion-MNIST case. Moreover,  $\bar{I}_B^M$  approaches -1 earlier when incremental mode is used. It is also approximately at the mentioned percentages where we see a decrease in test accuracy in Figure 1a and 1b in the incremental margin case. Thus, a network trained in incremental mode trains on more batches with low  $\bar{I}_B^M$ . This observation opens up for the hypothesis that the incremental training yields training with non-informative data which in turn causes the decrease of the test accuracy.

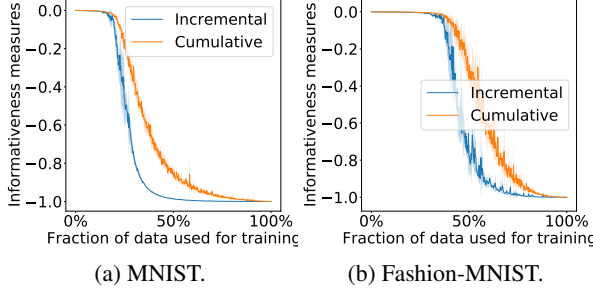


Figure 9: How the mean informativeness measure  $\bar{I}_B^M$  changes depending on training mode.

### A.3 Network Capacity

**Methodology.** In Section 3, we saw that the margin query strategy yields the best performance for the  $\text{ANN}_{100,1}$  network. Here, we investigate the different query strategies and training modes on networks of different capacities. The methodology of performing the experiments is consistent with the study in Section 3.

**Results and discussion.** Figure 10 shows the test accuracy of  $\text{ANN}_{10,1}$  and  $\text{ANN}_{1000,1}$  networks trained with the margin and entropy query strategies, where the batch size is 120. We report the results for both the incremental and cumulative training modes both on the MNIST and Fashion-MNIST data sets. The results on  $\text{ANN}_{100,1}$  are those reported in Figure 1.

In general, the results are consistent for different networks of varying capacities. The margin query strategy, trained with cumulative training, performs as good as or better than the random query strategy. It consistently outperforms the entropy query strategy.

The comparison between the incremental and cumulative training modes demonstrates consistent results: i) we observe a decline of the test accuracy of the networks trained with the incremental training mode, while the test accuracy of the networks trained with the cumulative mode increases as more data is fed to the network. ii) However, the incremental training mode may have an advantage at the early steps of the training which yields comparable or even better (with  $\text{ANN}_{10,1}$ ) results compared to cumulative training. This might explain why incremental training is used more often in practice, since active learning is sometimes concerned with labeling a small fraction of the total data.

When the capacity of the network is small, i.e., on  $\text{ANN}_{10,1}$ , the difference between the random and the margin query strategies is small for the cumulative training. Moreover, the difference in test accuracy between the incremental and cumulative training is more prominent for a smaller network, i.e., the decline of the test accuracy for a smaller network is more severe when using incremental training. The reason could be that a network with a smaller capacity is more sensitive to the bias induced by the training order caused by the specific query strategy. A larger network is more flexible due to its larger capacity.

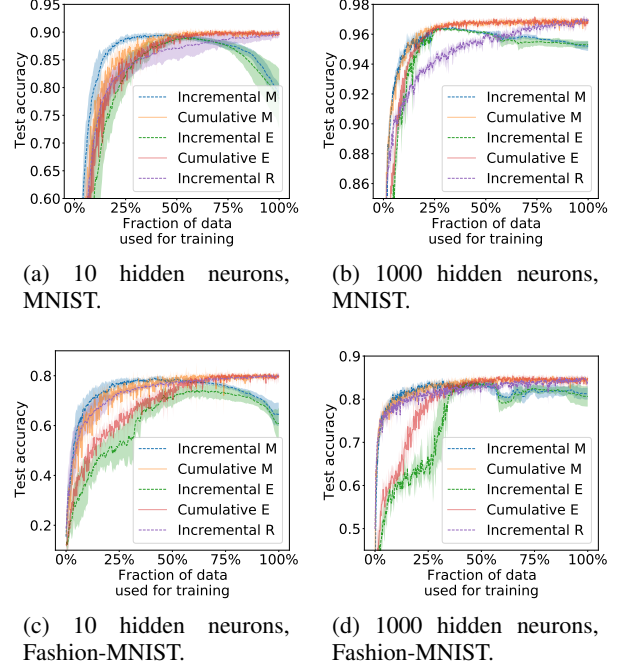


Figure 10: Performance of the random, margin, and entropy query strategies on  $\text{ANN}_{10,1}$  and  $\text{ANN}_{1000,1}$  networks with incremental and cumulative training modes.

### A.4 Choice of Batch Size

**Methodology.** The batch size  $n_B = |B|$  is the number of object labels queried together before (re)training the network at the next step. Ideally, to ensure that the most informative samples are labeled, only one object label should be queried per training step, i.e.  $n_B = 1$ . However, this slows down the training process. Instead,  $n_B$  samples with the lowest informativeness measures are selected. We thus study how  $n_B > 1$  affects the performance of the trained network for both the incremental and cumulative training modes.

**Results and Discussion.** Figure 11 illustrates the test accuracy for different choices of  $n_B$  for an  $\text{ANN}_{100,1}$  network. We investigate both the incremental and cumulative modes for selecting object labels with the margin query strategy. The results are averaged over 2 runs.

The results show that the choice of the batch size can affect the performance of the network and query strategy in particular when incremental training is used. The cumulative training mode seems less sensitive to the choice of  $n_B$ . The incremental training mode may be more affected by the choice of  $n_B$  since the class assumed to be the most informative may change during the training process. A large  $n_B$  may thus cause the network to train based on many objects wherein only one or few classes are represented. The cumulative training is not affected by a large batch size, presumably because it trains on all the available labeled data  $L$ . When the cumulative training mode selects a batch wherein only one or few classes are represented, the effect of the

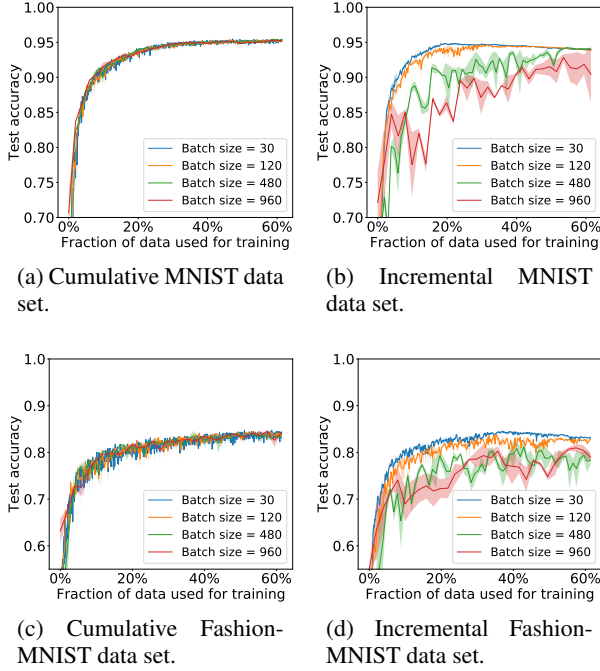


Figure 11: The test accuracy for a number of different batch sizes using an  $\text{ANN}_{100,1}$  network. The object labels are selected according to margin query strategy and the results are averaged over 2 runs.

choice of the selected batch will be diluted by the objects labeled previously.

In most of the studies in this paper, either a batch size  $n_B$  of 120 or a similar number such as 100 has been used. The results in Figure 11 show that different choices of  $n_B$  for cumulative training yield consistent results and the exact choice might not matter so much.

### A.5 Sample Distributions

**Methodology.** In Section 3, we observed that the margin strategy outperforms the random query strategy. We believe margin either samples a (1) good class distribution, i.e. it queries a suitable *multi* class distribution, containing objects from informative classes, (2) good *within* class distribution, i.e., the queried objects within one class are informative. For example, it samples objects close to the optimal decision boundaries.

We investigate the contribution of each of these two hypotheses by sampling and comparing three different subsets:

- Random sampling, which was sampled by the random query strategy.
- Margin sampled subset, denoted *QS sampled*, sampled by the margin query strategy.
- Resampled subset, which contains randomly sampled objects, weighted based on class label to ensure it has a similar class distribution as the QS sampled subset.

We use a cumulatively trained  $\text{ANN}_{100,1}$  to sample out 20000 of the 60000 objects in the MNIST and Fashion-MNIST data sets. Finally, an  $\text{ANN}_{100,1}$  network is trained on the sampled subsets to assess the performance on the corresponding test sets. We repeat this procedure 50 times.

**Results and discussion.** Figure 12a and 12c show the class distribution of the QS sampled and resampled subset. Figure 12b and 12d shows the test accuracy of  $\text{ANN}_{100,1}$  network associated with each subset. The highest test accuracy is given by the QS sampled subset. The resampled and randomly sampled subsets yield no significant difference in test accuracy on MNIST. The resampled subset outperforms the random sampling on Fashion-MNIST.

The results indicate that the distribution within the classes is the main factor to the improvement in test accuracy over random sampling. The distribution between the classes may contribute somewhat to the improvement in test accuracy but less significantly.

Finally, Figures 12a and 12c show that the margin query strategy samples classes that intuitively should be harder to distinguish. The most abundant classes are 9, 8, 5, 3, and 4 for the MNIST data set. For example, it is reasonable that a handwritten 4 is difficult to distinguish from a handwritten 9. Similarly, the most commonly sampled classes in the Fashion-MNIST data set are 0, 2, 4, and 6 with the respective class labels *T-shirt/top*, *Pullover*, *Coat*, and *Shirt* – classes which likely are difficult to distinguish by a human as well.

### A.6 Different Sizes for Random Start

In Section 6, we improved the performance of the entropy query strategy by using a random start of size 2000. Figure 13 shows a random start of size 200. We observe that although this random start improves the test accuracy, the used random start size is not sufficiently large to yield good performance. Thus, the random start size must be large enough to be effective.

Figure 14 shows additional experiments using the random start to estimate the test accuracy. The random start sizes are 600 and 3000, and the types of the networks are  $\text{ANN}_{100,1}$  and  $\text{ANN}_{100,5}$ . The results show that the upper and lower estimates are better after training on a large fraction on the unlabeled data. Using a random start of size 600 yields a larger variance compared to a random start of size 3000. Thus a sufficiently large random start is needed in order to make the estimates certain. However, a too large random start might yields a worse lower estimate.

When using one epoch, as shown in Figures 14a and 14c, the upper estimate is close to the real test accuracy. When using 5 epochs, as shown in Figures 14b and 14d, the upper estimate is considerably higher. This is natural since the more epochs help to learn more about the data. This directly affects the upper estimate, since the data is shared between the test set and the training set in this case. The upper estimate is thus worse if many epochs are used to train the model. Yet, we still think that this naive approach to estimate the test accuracy might be useful in some practical situations.

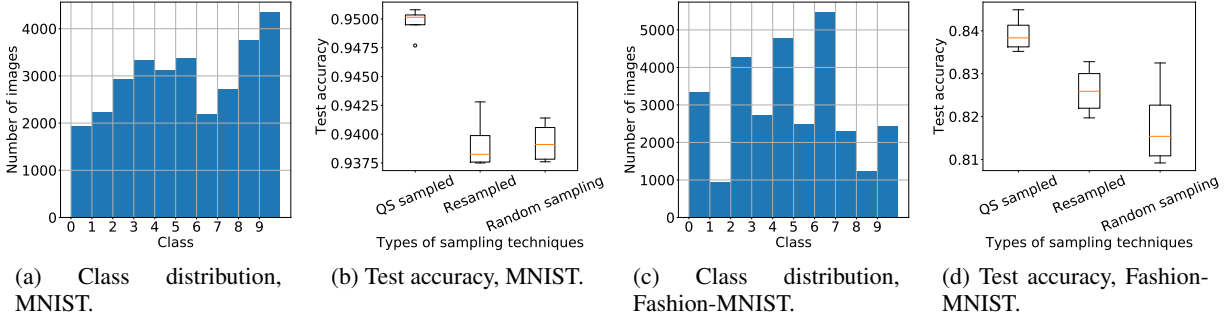


Figure 12: Class distribution if the QS sampled and resampled subsets for MNIST (a) and Fashion-MNIST (c). Test accuracy yielded by the three subsets for MNIST (b) and Fashion-MNIST (d).

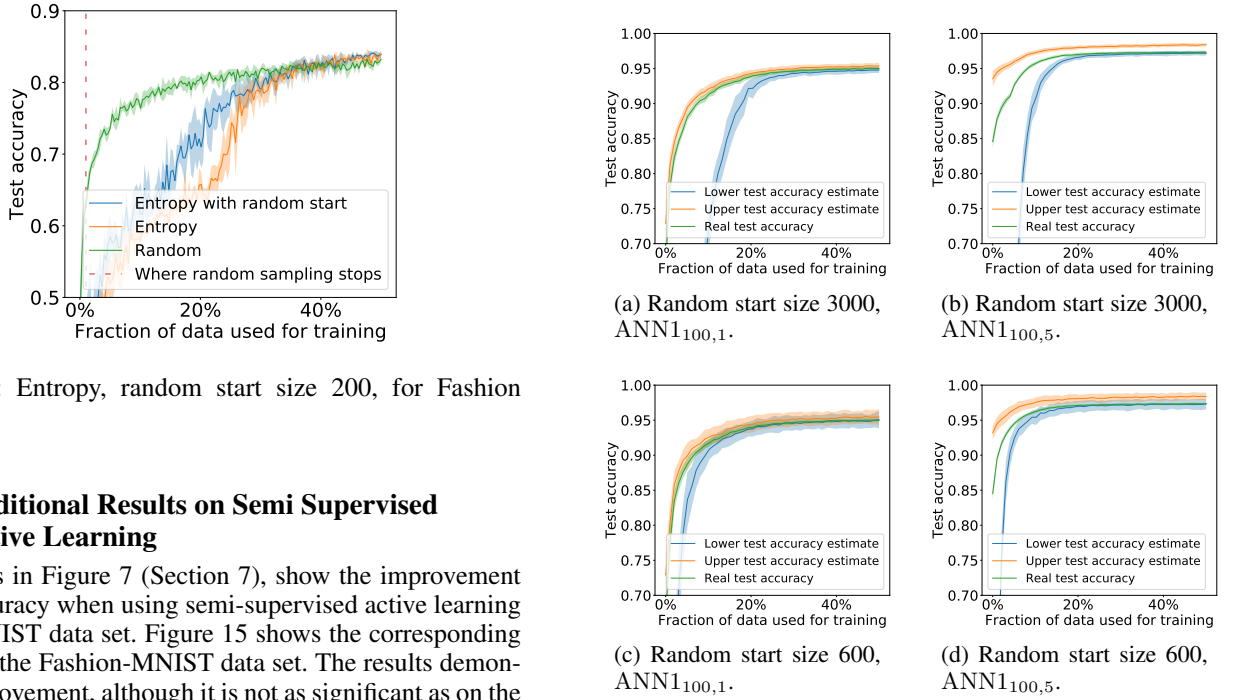


Figure 13: Entropy, random start size 200, for Fashion MNIST.

## A.7 Additional Results on Semi Supervised Active Learning

The results in Figure 7 (Section 7), show the improvement in test accuracy when using semi-supervised active learning on the MNIST data set. Figure 15 shows the corresponding results for the Fashion-MNIST data set. The results demonstrate improvement, although it is not as significant as on the MNIST data set.

## B Code

### B.1 Parameters for Training and Evaluation

Tensorflow's standard settings for the hyperparameters were used when training and evaluating the network, for the `model.fit()` function:

```
batch_size=32
validation_split = 0
validation_data=None
Shuffle = True
class_weight=None
sample_weight=None
initial_epoch=0
steps_per_epoch=None
validation_steps=None
validation_freq=1
```

```
max_queue_size=10
workers=1
use_multiprocessing=False
```

Tensorflow's standard settings for evaluation for the `model.evaluate()` function:

```
x=None
y=None
batch_size=None
verbose=1
sample_weight=None
steps=None
callbacks=None
```

Figure 14: Upper and lower test accuracy estimates for random start of different size and epochs on the MNIST data set, averaged over 50 different runs.

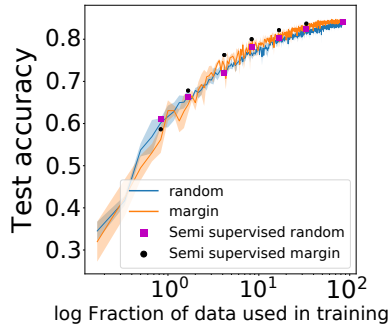


Figure 15: Test accuracy before and after semi-supervised active learning on Fashion MNIST.

```
max_queue_size=10
workers=1
use_multiprocessing=False
```

## B.2 Pseudo-Code Describing the $\text{ANN}_{m,e}$ Network

```
model = tf.keras.models.Sequential([
    Flatten(input_shape = (28,28)),
    Dense(m, activation='relu'),
    Dropout(0.2),
    Dense(10, activation='softmax')
])
model.compile(optimizer='adam',
              loss='sparse_categorical_crossentropy',
              metrics=['accuracy'])
```

The dropout operation randomly removes 20% of the network parameters during training, to reduce the risk of overfitting. The weight parameters are initialized according to the Glorot uniform distribution and the bias parameters are initialized by zero. We use the Adam optimiser (Kingma and Ba 2015) with the default learning rate of  $10^{-3}$  to train the network.  $e$  epochs are used for training.

## B.3 Pseudo-Code Describing the CNN1 Network

50 epochs are always used for training. Conv2D always has the properties of

```
activation='relu',
kernel_initializer='he_uniform',
padding='same'
```

```
model =
tf.keras.models.Sequential()
Conv2D(32, (3, 3),
input_shape=(32, 32, 3))
Conv2D(32, (3, 3))
MaxPooling2D((2, 2))
Dropout(0.2)
Conv2D(64, (3, 3))
Conv2D(64, (3, 3))
MaxPooling2D((2, 2))
Dropout(0.2)
```

```
Conv2D(128, (3, 3))
Conv2D(128, (3, 3))
MaxPooling2D((2, 2))
Dropout(0.2)
Flatten()
Dense(128, activation='relu',
kernel_initializer='he_uniform')
Dropout(0.2)
Dense(10, activation='softmax')
```

```
opt = tf.keras.optimizers.SGD
(lr=0.001, momentum=0.9)
model.compile(
optimizer=opt,
loss=
'categorical_crossentropy',
metrics=['accuracy'])
```